

Computing the shielding effectiveness of waveguides using FE-mesh truncation by surface operator implementation

C. Tuerk*, W. Renhart†, and C. Magele†

*Armament and Defence Technology Agency, Ministry of Defence and Sports, Rossauer Laende 1, A-1090 Vienna

† Institute for Fundamentals and Theory in Electrical Engineering, Inffeldgasse 18, A-8010 Graz

E-mail: christian.tuerk@bmlvs.gv.at

Abstract—A plane wave incident perpendicular to one open end of a conductive tube, as part of a honeycomb-structure, is attenuated on its way through it. In order to calculate its total attenuation for various frequencies the FE-method will be used. This requires a reflectionless truncation of the FE-mesh for which a Surface Operator Boundary Condition (SOBC) will be employed. In order to show the accuracy and applicability of the FEM with SOBC, the results will be compared to entirely analytical solutions as well as to easy-to-use engineering formulae.

Index Terms—Finite Element Method (FEM), Shielding, Surface Operator Boundary Condition (SOBC), Waveguide

I. INTRODUCTION

Previous works i.e. [1] have shown the implementation of a surface operator boundary condition derived from an analytical model into the FE-mesh. Honeycombs can be considered waveguides-beyond-cutoff (WBC) and are therefore employed as vents for large shielded enclosures, like shielded rooms, while maintaining a certain degree of attenuation of a plane wave incident on it.

The resulting attenuation imposed by a single conductive tube will be calculated under different ratios of length-to-diameter of the tube and at selected frequencies.

Existing literature like [2] provide engineering rules for designing waveguides-beyond-cutoff (WBC) as a shielding component whereas others like [3] present analytical details on the physics of the transmission of electromagnetic power in waveguides of various cross-sections. The results, obtained through numerical computation in the frequency range of $3GHz$ to $18GHz$ for a practical design of a real life waveguide are then compared to both approaches and subsequently discussed.

II. MODELLING

A. Surface Operator Boundary Conditions (SOBC)

Fig. 1 shows the setup used for the computation of the plane wave field strength incident on the tube and exiting it. The right-hand-side boundary is modelled by means of SOBCs (Γ_{tr}) matching the impedance of free space between the tube and the termination of the problem area. A plane wave travelling along the x-axis will experience a certain degree of attenuation by the waveguide as long as the waveguide-beyond-cutoff (WBC) condition is met. A fraction of the initial power of the wave penetrates the waveguide and is terminated reflectionless at Γ_{tr} .

Based on results obtained through [5] and [4] the implementation of this surface operator boundary condition for the truncation surface Γ_{tr} of the FE-mesh can be directly derived from the Maxwell equations

$$\nabla \times \vec{E} = -j\omega\mu\vec{H}, \quad \nabla \times \vec{H} = j\omega\epsilon\vec{E}. \quad (1)$$

After splitting the field vectors \vec{E} and \vec{H} as well as the ∇ -operator into their normal and orthogonal tangential

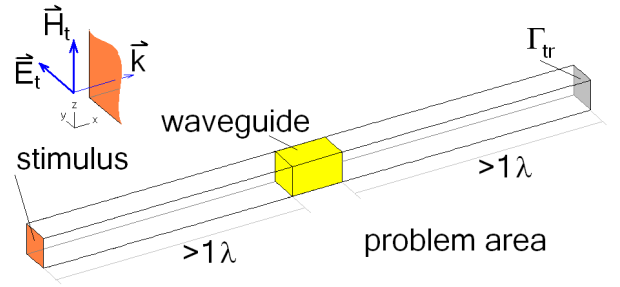


Fig. 1. Modelling the Waveguide

components as in 2

$$\vec{E} = \vec{E}_t + \vec{n}E_n, \quad \vec{H} = \vec{H}_t + \vec{n}H_n, \quad \nabla = \nabla_t + \frac{\partial}{\partial n}\vec{n} \quad (2)$$

the Maxwell Equations can be reformulated as follows:

$$\vec{n}\vec{H}_n = -\frac{1}{j\omega\mu}\nabla_t \times \vec{E}_t \quad (3)$$

$$\vec{n}\vec{E}_n = \frac{1}{j\omega\epsilon}\nabla_t \times \vec{H}_t. \quad (4)$$

With these relations the normal components of the field components E_n and H_n can be eliminated in equation 1. A couple of mathematical operations finally yield

$$\frac{\partial(\vec{n} \times \vec{E}_t)}{\partial n} = -j\omega\mu\vec{H}_t - \frac{1}{j\omega\epsilon}\nabla_t \times (\nabla_t \times \vec{H}_t) \quad (5)$$

$$\frac{\partial(\vec{n} \times \vec{H}_t)}{\partial n} = j\omega\epsilon\vec{E}_t + \frac{1}{j\omega\mu}\nabla_t \times (\nabla_t \times \vec{E}_t). \quad (6)$$

These equations are commonly valid, consequently on the truncation surface (see fig. 1) too. On Γ_{tr} the situation is as shown in fig. 2 in a local coordinate system. The propagation of the wave can be represented by the wave vector \vec{k} . Due to the knowledge of the angle of incidence on Γ_{tr} it can be decomposed into its normal and tangential components as given in the following set of equations:

$$\vec{k} = \vec{k}_t + \vec{\beta}, \quad \beta = \pm\sqrt{k^2 - k_t^2}, \quad k = \omega\sqrt{\mu\epsilon}. \quad (7)$$

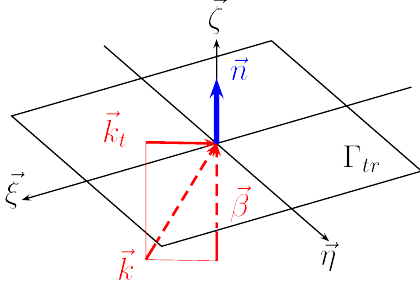


Fig. 2. Wave at any point on Γ_{tr} .

The surface normal \vec{n} is represented by the local coordinate $\vec{\zeta}$. In order to get rid of the $\frac{\partial}{\partial \vec{n}}$ term on the left-hand-side of equation 5 and equation 6 an integration along ζ over the half-space must be performed. Assuming a lossy media, the field components must decay to zero at infinity which allows for

$$\int_{\zeta=0}^{\infty} \vec{H}_{t0} e^{-j\beta\zeta} d\zeta = \frac{1}{j\beta} \vec{H}_{t0} \quad (8)$$

$$\int_{\zeta=0}^{\infty} \vec{E}_{t0} e^{-j\beta\zeta} d\zeta = \frac{1}{j\beta} \vec{E}_{t0}.$$

\vec{H}_{t0} and \vec{E}_{t0} are the tangential field vectors at $\zeta = 0$. Together with equation 7, relations 5 and 6 can now be rewritten as

$$\vec{n} \times \vec{E}_{t0} = \frac{-\omega\mu\vec{H}_{t0}}{\sqrt{k^2 - k_t^2}} + \frac{\nabla_t \times (\nabla_t \times \vec{H}_{t0})}{\omega\epsilon\sqrt{k^2 - k_t^2}} \quad (9)$$

$$\vec{n} \times \vec{H}_{t0} = \frac{\omega\epsilon\vec{E}_{t0}}{\sqrt{k^2 - k_t^2}} - \frac{\nabla_t \times (\nabla_t \times \vec{E}_{t0})}{\omega\mu\sqrt{k^2 - k_t^2}}. \quad (10)$$

Transverse components of the outgoing wave may be transformed into the Fourier domain, only to see, that its tangential derivatives can be expressed as $\nabla_t = -jk_t$. Substitution in equation 9 and 10 leads to

$$\vec{n} \times \vec{E}_{t0} = \frac{-\omega\mu\vec{H}_{t0}}{\sqrt{k^2 - k_t^2}} - \frac{\vec{k}_t \times (\vec{k}_t \times \vec{H}_{t0})}{\omega\epsilon\sqrt{k^2 - k_t^2}} \quad (11)$$

$$\vec{n} \times \vec{H}_{t0} = \frac{\omega\epsilon\vec{E}_{t0}}{\sqrt{k^2 - k_t^2}} + \frac{\vec{k}_t \times (\vec{k}_t \times \vec{E}_{t0})}{\omega\mu\sqrt{k^2 - k_t^2}}. \quad (12)$$

These relations between the tangential components of \vec{E}_{t0} and \vec{H}_{t0} can now be used to model the so called surface operator boundary conditions (SOBC) on Γ_{tr} . Equations 11 and 12 allow for any angle of incidence of the plane wave on a truncating surface Γ_{tr} . Since only perpendicular incidence on the waveguide and on Γ_{tr} are considered, the use of a first-order SOBC is reasonable - $\vec{k}_t = 0$.

Application of the Galerkin method to the well-known \vec{A}, v -formulation makes use of the $\vec{n} \times \vec{H}_t$ on the Neu-

mann Boundary (see [6]).

$$-\int_{\Omega} \nabla \times \vec{N}_i \cdot \frac{1}{\mu} \nabla \times \vec{A} d\Omega + \int_{\Gamma_H} \vec{N}_i \cdot \underbrace{\left(\vec{n} \times \left(\frac{1}{\mu} \nabla \times \vec{A} \right) \right)}_{\vec{n} \times \vec{H}} d\Gamma + \int_{\Omega} \vec{N}_i \cdot (\sigma + j\omega\epsilon) j\omega (\vec{A} - \nabla v) d\Omega = 0. \quad (13)$$

On the Neumann boundary (Γ_H) the underbraced term in equation 13 is substituted by the Fourier transformed integral of equation 6 which prescribes the truncation of the FE-mesh directly.

B. Surface Impedance Boundary Conditions (SIBC)

An increased incident angle results always in a larger wave vector \vec{k}_t and obviously the curl curl-terms in equations 11 and 12 become more and more relevance to achieve accurate boundary conditions. If the wave propagates perpendicularly to Γ_{tr} , the vector \vec{k}_t equals zero. This is the considered case for all results presented herein. Hence the second term on the right-hand-side in equations 11 and 12 equal zero and first order SIBCs remain:

$$\vec{n} \times \vec{E}_{t0} = \frac{-\omega\mu\vec{H}_{t0}}{k} = -\sqrt{\frac{\mu}{\epsilon}} \vec{H}_{t0} = -Z_0 \vec{H}_{t0} \quad (14)$$

$$\vec{n} \times \vec{H}_{t0} = \frac{\omega\epsilon\vec{E}_{t0}}{k} = -\sqrt{\frac{\epsilon}{\mu}} \vec{E}_{t0} = \frac{1}{Z_0} \vec{E}_{t0} \quad (15)$$

The impedance of the mesh-terminating plane Γ_{tr} can now be directly prescribed.

III. SETUP

Fig. 1 shows the setup used for the computation of the plane wave field strength incident on the tube and exiting it. The right-hand-side of the problem area is terminated by means of the introduced SOBC. A plane wave originating from the stimulus plane penetrates the tube. Only a fraction of the incident power "leaks" through it, since at the frequencies considered it represents a waveguide-beyond-cutoff (WBC). This small fraction of the incident wave is terminated reflectionless at Γ_{tr} . The detail of the aluminium tube with a square cross-section and lengths ranging from 20mm ... 80mm is shown in fig. 3.

The grid shown in figure 3 represents the macro elements used for modelling only.

IV. RESULTS

A. Finite Element Method with SOBC

Since frequencies above 1GHz are of interest, simulations at distinct frequencies in the range of 3 ... 18GHz at a stepwidth of 3GHz are considered. At each frequency the length of the tube is stepped through by 10mm in the range between 20mm and 80mm. The cross-section of the waveguide is kept constant. Fig. 4 shows the resulting attenuation of a plane wave on its way through

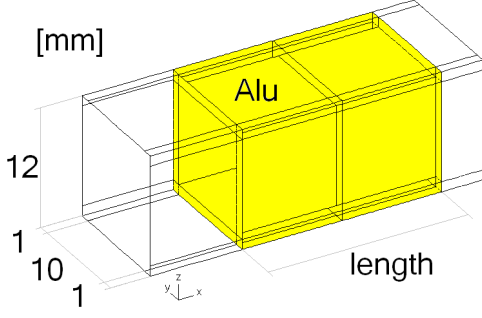


Fig. 3. Details of the waveguide-beyond-cutoff

the WBC. At $15GHz$ the attenuation of the incident wave starts to approach zero and the tube becomes a waveguide as known from RF-applications and has also been described in [3]. As long as the frequencies are

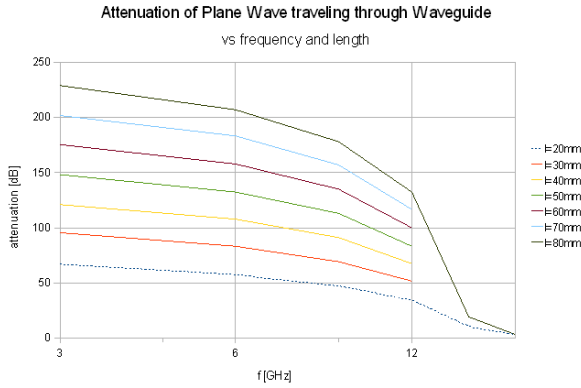


Fig. 4. Attenuation of a plane wave at distinct lengths and frequencies

below the cutoff-frequency, the attenuation does not only depend on the ratio between f , the frequency used, and the cutoff-frequency f_c of the structure, but also depends on the length of the tube. The relationship is non-linear and therefore clearly contrasting the engineering rules-of-thumb as provided in the following section.

The following figure (Fig. 5) shows the computation of the field strengths on either side of the waveguide-beyond-cutoff. It is operated at $9GHz$ and the right-hand-side is terminated by means of the SOBC described before. The colors in the figure refer to the absolute value of the field strengths of the electrical component of the plane wave at a particular moment. Due to the necessity of a fine mesh for the computation of fields along the waveguide (coloured grey), no field strengths are visible. Following the general formula of the power density of a plane wave

$$S = \frac{1}{2} \text{Re}(\vec{E} \times \vec{H}^*) \quad (16)$$

and the impedance of free space of

$$Z_0 = \sqrt{\frac{\mu_0}{\epsilon_0}}$$

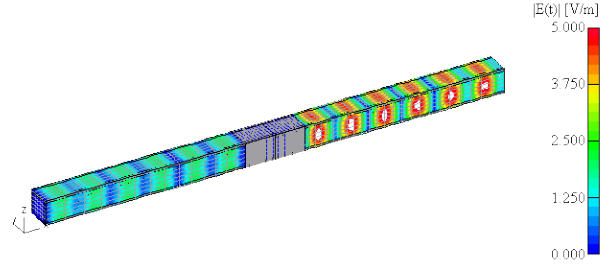


Fig. 5. A waveguide 30mm in length, operated at $9GHz$

the attenuation of the power through the waveguide can be calculated. With

$$a_t = 20 \lg \frac{|E_{maxin}|}{|E_{maxout}|} \quad (17)$$

the degree of the attenuation (a_t) [dB] can be determined based on the field strength of the electrical component of the plane wave on the left-hand-side of the tube ($|E_{maxin}|$) and on the right-hand-side ($|E_{maxout}|$). The maxima of the respective field strengths are taken from a line parallel to the x-axis along the centre of the tube.

B. Engineering Rules

For applications using frequencies below approximately $1GHz$ [2] proposes the use of simple "design rules":

$$f_c = \frac{150}{b}, \quad f_c [GHz], \text{ diameter} [mm] \quad (18)$$

$$a_t = \frac{27.3}{b} l, \quad a_t [dB], \text{ diameter, length} [mm] \quad (19)$$

$$b = \sqrt{2}a, \quad \text{forsquare cross - section} [mm]$$

$$f \leq \frac{f_c}{10}, \quad \text{usable frequency} \quad (20)$$

with f_c being the cutoff-frequency in [GHz], a_t representing the shielding effectiveness in [dB] and any dimension given in [mm]. Formulae 18 to 20 show that the cutoff-frequency only depends on the diameter of the tube which is, to some degree, in accordance with [3]. It has to be distinguished whether a square, rectangular or circular waveguide is used. As for the rectangular cross-sections [3] reads that the larger dimension governs the cutoff-frequency f_c . For circular shapes the diameter counts. One may also have noticed that the engineering rules do not account for any matter in the waveguide but free space. Since the WBC is used as a vent with shielding properties its cutoff-wavelength follows

$$\lambda_c = \frac{c_0}{f_c} \approx 2a. \quad (21)$$

This is in line with [3] and equation 22 if $\epsilon = \epsilon_0$ and $\mu = \mu_0$. Waveguides filled with dielectric matter for transmission properties are beyond the scope of this work since they are neither useful as vents nor as a shielding component.

As long as the frequency of interest is below the highest usable frequency as given in equation 20 the tube yields an attenuation according to equation 19. Application of this set of formulae to the waveguide under consideration at $12GHz$ provides the following graph (fig. 6):

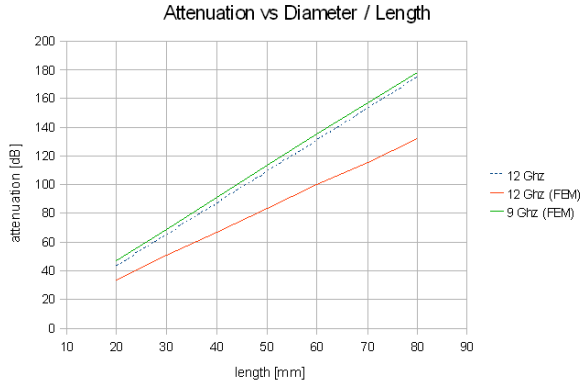


Fig. 6. Engineering rules applied at $12GHz$

Figure 6 shows the application of the engineering rules at the cutoff-frequency $f_c = 12GHz$. The calculation of the shielding effectiveness with the engineering rules (blue dashed line) naturally exceed the limits obtained by means of the numerical value since equation 20 has not been considered so far. This equation is obviously a very rough estimate of the maximum usable frequency. It requires this waveguide not to be used above $1.2GHz$. This is very conservative, since the green solid line (the uppermost line) shows the course of the shielding effectiveness at $9GHz$ of this particular waveguide. The engineering rules yield similar results, but on the safe side. Since it is not clear which limit in terms of shielding effectiveness underlies this set of easy-to-use engineering rules, one has to be very careful with its application. Even if it was possible to adjust equation 20 to this result, the behaviour of a waveguide may render this unreliable due to its nonlinear attenuation of a plane wave as fig. 4 clearly shows.

C. Analytical Approach

When considering a waveguide-beyond-cutoff (WBC) for shielding purposes, the lowest mode of a TE or TM-wave propagating through it is of interest. It represents the cutoff-frequency f_c . For waveguides with a square cross-section [3] reads for TE_{10} -mode

$$f_c = \frac{1}{2\sqrt{\epsilon\mu}} \frac{1}{a} \quad (22)$$

with a being the length of the edge of the square. For a waveguide as used for this work, $f_c = 14.99GHz$ which matches the result shown in figure 4. With increasing frequencies the attenuation of the plane waves vanishes above approximately $15GHz$ regardless of the length of it. In other words, illuminating this particular waveguide at frequencies $\geq 15GHz$ will render it useless as a shield.

Since waveguides are generally used for transmission of electromagnetic energy there are, apart from the engineering rules above, no analytical formulations available to determine the attenuation of a plane wave penetrating a waveguide below its cutoff-frequency - there is no distinct mode of energy flow in the waveguide. For the same reason there are no analytical formulations known for plane waves penetrating a waveguide at other angles than perpendicular to the cross-section of it (see section V).

V. CONCLUSION

This paper shows how Surface Operator Boundary Conditions (SOBC) can be implemented in an $\vec{A} - v$ formulation to be used with the Galerkin method. The SOBC are used to model a Neumann Boundary Condition which allows for reflectionless termination of a problem area. The use of the SOBC allows for a significant speed-up of the computation of the problem because the absorbing boundary is only a single term which does not require additional finite elements to be modelled. For the construction of vents in a shielded room, waveguides below their cutoff-frequencies are employed. The described model has been used for the computation of the shielding effectiveness of waveguides at frequencies exceeding $1GHz$ and compared and contrasted to an analytical approach and a set of easy-to-use engineering rules. It can now clearly be shown, that well known and verified analytical solutions can be met by numerical models as far as the cutoff-frequency of square waveguides is concerned. By the same token, it can be shown that simple design rules are very conservative i.e. delivering smaller numbers of shielding attenuation than actually can be yielded in real designs. It can not be said, that this set of easy-to-use rules are valid only below $\approx 1GHz$.

So far, only plane waves incident perpendicular to an open end of the waveguide have been modelled and computed. Future efforts will be put on different angles of incidence. There exist hints, that stacked arrays of waveguides (honeycomb structures) suffer a deterioration of total shielding effectiveness compared to the attenuation provided by a single tube. This behaviour may also be investigated in the future.

REFERENCES

- [1] W. Renhart, C. Magele and C. Tuerk, "Thin Layer Transition Matrix Description Applied to the Finite Element Method", IEEE Trans on Magn., Vol. 45, No. 3, 2009, pp. 1638- 1641.
- [2] Louis T. Gnecco, "The Design of Shielded Enclosures", Newnes Press, ISBN 0-7506-7270-6
- [3] Karoly Simonyi, "Theoretische Elektrotechnik", 6. Auflage, VEB Deutscher Verlag der Wissenschaften, Berlin 1977
- [4] W. Renhart, C. Magele and C. Tuerk, "Improved FE-mesh truncation by surface operator implementation to speed up antenna design" (unpublished).
- [5] Sergei Tretyakov, Analytical Modeling in Applied Electromagnetics, 1st ed. Artech House, chapters 2, 3, 2003.
- [6] O. Biro, "Edge element formulations of eddy current problems", Computer methods in applied mechanics and engineering, vol. 169, pp. 391-405, 1999.